View Online / Journal Homepage / Table of Contents for this issue
Dynamic Article Links

Nanoscale

Cite this: *Nanoscale*, 2012, **4**, 6955

www.rsc.org/nanoscale

COMMUNICATION

Laser patterning of conductive gold micronanostructures from nanodots†

Bin-Bin Xu,[a] Ran Zhang,[a] Huan Wang,[a] Xue-Qing Liu,[a] Lei Wang,[a] Zhuo-Chen Ma,[a] Qi-Dai Chen,*[a] Xin-Ze Xiao,[a] Bing Han[a] and Hong-Bo Sun*[ab]

Received 25th June 2012, Accepted 26th August 2012
DOI: 10.1039/c2nr31614e

Published on 28 August 2012 on http://pubs.rsc.org | doi:10.1039/C2NR31614E
Downloaded by Jilin University on 31 October 2012

Gold nanodots were used as the precursory material to form micronanopatterns under pinpoint scanning by a tightly focused femtosecond laser beam. Different from the widely reported metal ions photoreduction mechanism, here gradient force in an optical trap generated around the laser focus is considered as the major mechanism for particle accumulation (focusing). It has been proven to be an effective method for gold micronanostructure fabrication, and the electronic resistivity of the resulting metals reached as high as 5.5×10^{-8} Ω m, only twice that of the bulk material (2.4×10^{-8} Ω m). This merit makes it a novel free interconnection technology for micronanodevice fabrication.

In recent years, metal micro/nano structures have attracted extensive research attention because they are the key elements for use in the following: plasmonic optical antennas,[1] plasmon resonance energy transfer,[2] concentration of light to enhance the optical response to nearby molecules such as surface enhanced Raman scattering (SERS),[3] highly efficient three component coupling reactions,[4] colorimetric and fluorescent detection of ions and small organic molecules,[5] and especially in electronic industry applications such as interconnection in single-molecule devices, carbon nanotube (CNT) devices and DNA tubes.[6] Usual technologies for fabricating metal structures, *i.e.*, UV-lithography, E-beam lithography (EBL), and focused ion beam etching (FIB) need expensive vacuum conditions, complex technical steps or sometimes toxic chemicals, and photoresistors or carrier gases may destroy CNT or functional molecular parts,[7] leading to low performance or even failure of devices. Two-photon absorption (TPA) processing technology[8] has been developed for producing conductive metal micronanostructures in one step and under gentle conditions. Typically, silver wires or complex structures were fabricated through TPA induced photochemical reactions by using appropriate salt solutions as the precursory source[8e,9] and adding photosensitive molecules[9a,10] as the photoinitiator. For example, Kawata *et al.* reported fabrication of electrically conductive silver wires with a minimum width of 400 nm and three-dimensional (3D) silver microstructures by using silver nitrate aqueous solution with coumarin 440 as a two-photon sensitive dye. Some of the current authors demonstrated a flexible 3D nanowiring approach with a minimum wire width of 125 nm for electronic connections on nonplanar substrates by using silver ions as both metal source and photoinitiator.[9d] However, silver structures were instable and a silver sulfide film tended to form when exposed to air. Though gold micro/nano structures are more stable and antioxidant, there are only a few examples of TPA induced fabrication of gold structures,[8e,10] most of which were based on photoreduction of gold ions inside polymer films. The resulting structures are generally not electronically conductive. In this communication, we developed an alternative femtosecond laser direct writing method that relies on the usage of metal nanodots[11] as precursory source instead of metal ions. The previous work was based on the *in situ* optical reduction to form metal atoms, however not all of the metals or other materials could be reduced *in situ*. We report the first preparation of good conductive gold wires and complicated structures that were created in one step through directly depositing nanodots from colloidal suspension, and assembling and fusing the nanodots to pattern desired microstructures, during which no reduction process was involved. The gold microwires were applied for the electric connection of carbon nanotube devices.

The gold nanodots were synthesized in biphasic reaction conditions.[11] Tetraoctylammonium bromide (0.75 g, 2.75 mmol) was dissolved in 40 mL toluene, and hydrogen chloroaurate trihydrate (0.16 g, 0.81 mmol) was dissolved in 5 mL water. The two solutions were mixed together with stirring for 5 min. Then the aqueous phase was discarded from the flask after hydrogen chloroaurate was completely transferred into the organic phase. Hexanethiol (0.21 mL) was added before 10 mL freshly prepared aqueous sodium borohydride (0.14 g, 7.4 mmol) solution was rapidly injected into the flask, and the solution color soon became dark purple. The aqueous phase was removed again after 3 h of reaction. The remaining organic solvent was removed using a rotary evaporator. The black solid product was washed five times with methanol using centrifugal method and dried with nitrogen completely. Finally, the black powder was dissolved in toluene for use. The average diameter of nanodots in the biphasic reaction is between 1.5 nm and 4 nm, which are smaller than the ones synthesised by the Na_3-citrate reduction

[a]*State Key Laboratory on Integrated Optoelectronics, College of Electronic Science and Engineering, Jilin University, 2699 Qianjin Street, Changchun, 130012, People's Republic of China. E-mail: chenqd@jlu.edu.cn; hbsun@jlu.edu.cn; Fax: +86-431-85168281; Tel: +86-431-85168281*
[b]*College of Physics, Jilin University, 119 Jiefang Road, Changchun, 130023, People's Republic of China*

† Electronic supplementary information (ESI) available: Characterization, calculation of gradient optical force, the thermal characteristics of the gold nanodots, resistivity characterization of laser created gold wire, the stable electrical property of gold microstructures. See DOI: 10.1039/c2nr31614e

Published on 28 August 2012 on http://pubs.rsc.org | doi:10.1039/C2NR31614E
Downloaded by Jilin University on 31 October 2012

method in single phase[12] [transmission electron microscopy (TEM) in Fig. 1a and b]. The inset of Fig. 1a is the selected area electron diffraction (SAED) pattern of nanodots, indicating their polycrystalline structures. The bright rings correspond to the (111), (200), (220) and (311) planes of gold, consistent with the X-ray diffraction (XRD) analysis (Fig. 1c). The most significant diffraction peak at 38.2° corresponds to the (111) orientation, and it was confirmed by the high-resolution transmission electron microscopy (HRTEM) image (Fig. 1b).

The gold nanodots suspension was dropped onto the surface of cover glass and the sample was placed in the femtosecond laser direct writing system (FsLDW). 800 nm femtosecond laser pulses, with a width of 120 fs, were tightly focused on the interface between substrate and solution by a high numerical aperture oil-immersion objective lens (NA = 1.35, 100×).[9d,13] The optical forces induced the patterning process through deposition and aggregation in the laser focused area and the scheme of the laser patterning fabrication process is shown in Fig. 2a. The optical forces were widely used to trap and manipulate dielectric nanoparticles in the initial research. In the optical trapping technique a microdielectric object with a higher refractive index than a surrounding liquid is trapped near the focal point of a laser beam, whereas an object with a lower refractive index is subjected to a repulsive force from the focused beam.[14] However, it is shown that the trapping efficiency of a Rayleigh (diameter $d \ll$ wavelength λ) gold particle is 7 fold better than a similar-sized latex particle. Generally, the optical forces exerted on a metallic Rayleigh particle in an optical trap include absorption force, scattering force and gradient force. For very tiny particles the scattering and absorption forces are negligible in comparison to the gradient force.[15] Herein, the nanodot size ranges between 1.5 and 4 nm, the gradient force was the dominant factor and is expressed as follows,

$$F_{\text{grad}} = \frac{|\alpha|}{2}\nabla\langle E^2\rangle \quad (1)$$

where α is the polarizability of a nanodot and E is the optical electric field vector. The optical trapping range of metal nanoparticles has been expanded from a few nanometers to hundreds of nanometers

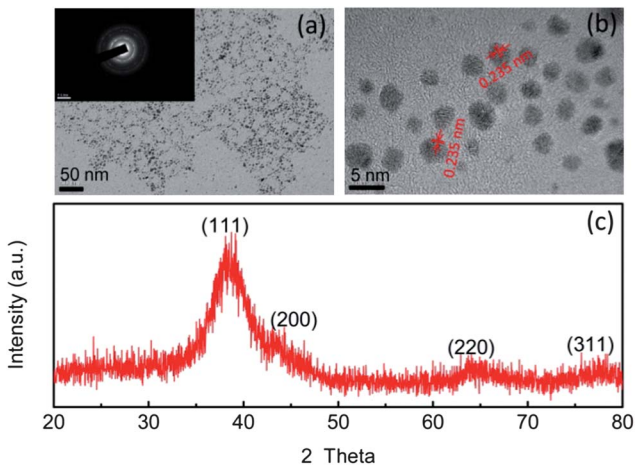

Fig. 1 Gold nanodots were synthesized through biphasic reaction. (a) TEM of nanodots, the inset is the SAED pattern of nanodots. (b) HRTEM of nanodots with the interplanar value of 0.235 nm corresponding to the (111) orientation. (c) XRD spectrum of gold nanodot powder.

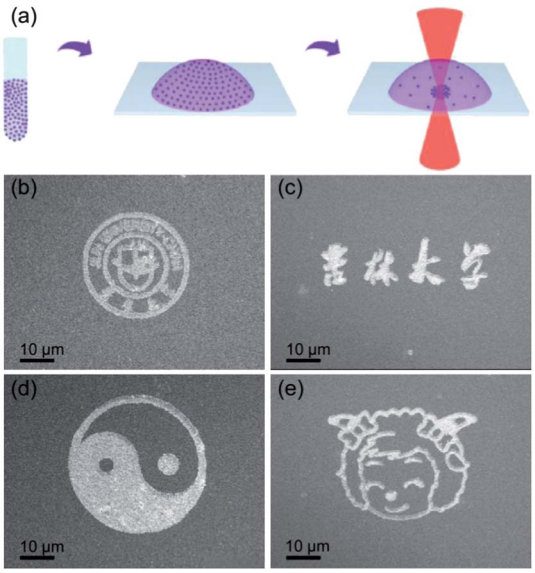

Fig. 2 Laser patterned gold micropatterns from colloidal gold nanodots. (a) Scheme of laser patterning fabrication process. (b–e) SEMs of laser patterned gold micropatterns including badge, Chinese characters of Jilin University, Tai Chi and cartoon sheephead.

and a few tens of milli-watts of laser power can produce pico-Newton (pN) range forces.[15b] When we applied ten milli-watts of laser power, the maximum gradient force was 7.28 pN (calculation details shown in ESI†) and sufficient for particle accumulation or focusing. Experimentally, controlled amounts of momentum were applied to the nanodots, breaking the equilibrium in solution phase and expelling nanodots from colloidal suspension to aggregate and deposit on the designated site on the substrate. The optical gradient force takes a major role in driving and pattering the metal nanodots on the substrate. In addition, the light-heat effect would influence the surface morphologies of gold micronanostructures and some bigger nanoparticles formed on the surface. The melting temperature of the gold nanodots was around 190 °C, examined by thermogravimetric analysis (TGA) and differential scanning calorimeter (DSC). When we applied enough laser power, the corresponding heat generated would make the nanodots fuse and form even bigger nanoparticles (Fig. 2b–e) on the pattern surface. In conclusion, the optical gradient force plays a major role in driving and pattering the metal nanodots on the substrate and the light-heat effect influences the surface morphologies, including roughness and specific ripples (Fig. 3a and c), of gold microstructures.

The immobilization occurred due to the van der Waals attracting interaction (F_{vdW}) between nanodots and substrate.[16]

$$F_{\text{vdW}}(z) = \frac{2Ar^3}{3z^2(z+2r)^2} \quad (2)$$

where z is the distance from the surface, r is the partical radius, A is the Hamaker constant. The surfaces of gold nanodots with negative charges due to the tiny residual thiol group would also generate an attraction effect to the substrate. Different micronanopatterns were formed according to the computer program laser scanning route and the residual gold suspension would be carefully removed. The unique arbitrary-shape designability of the FsLDW system ensured the patterning fabrication of complex configurations and gold

This journal is © The Royal Society of Chemistry 2012

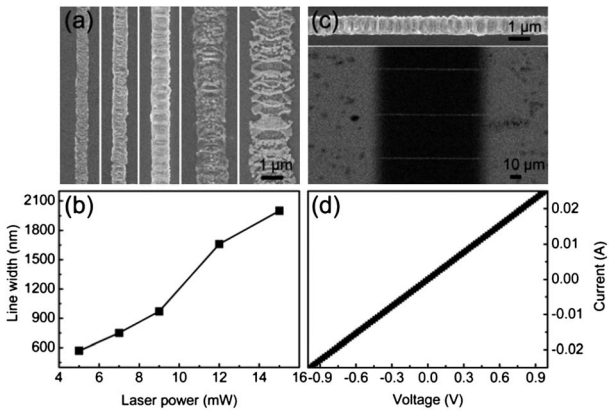

Fig. 3 Gold micronanowires were fabricated by laser patterning nanodots. (a) SEM of gold wires of different widths. (b) Dependence of wire width on the laser power. (c) SEM image of gold microwire between two Au–Ge–Ni electrodes. (d) Current–voltage curve of the two gold microwires.

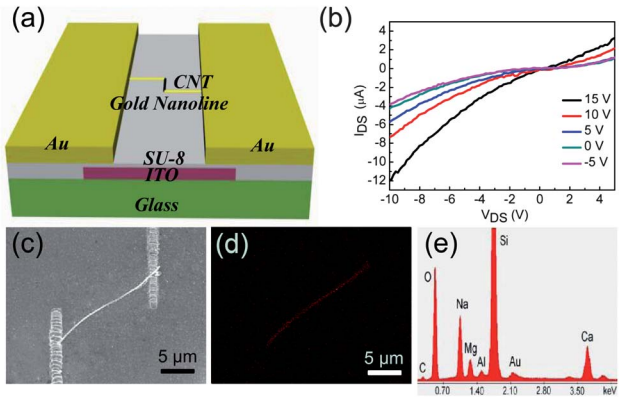

Fig. 4 Flexibility of laser patterning micronanowires served as conductive leads for a single MWCNT-FET device. (a) Scheme of bottom gate MWCNT-FET. (b) Output characteristics of MWCNT-FET. (c–e) SEM of gold wires connecting carbon nanotubes, the corresponding C element distribution by EDX and EDX spectrum.

micropatterns like badge, Chinese characters of Jilin University, Tai Chi pattern and cartoon sheephead, as shown in Fig. 2b–e.

To optimize the laser patterning fabrication condition, we carefully evaluated the dependence of fabrication resolution on the laser power. As shown in Fig. 3a and b, we fabricated a series of gold microwires on the cover glass under different laser powers and found the width increased with laser power increase. The thinnest wire is about 560 nm wide when the laser power was 5 mW. This dependence phenomenon is similar to the femtosecond laser induced photoreduction of silver wires,[9d] both were on account of the combinative effect of nonlinear light–matter interactions, *i.e.*, the square dependence of the absorption rate on the laser intensity and the threshold response of the metal salt solution to the light excitation.[8a] However, the corrugated surface of microwires was formed by laser induced evaporation of toluene in dot by dot scanning method. Too large a laser power leads to rapid evaporation of toluene even forming bubbles which could make the gold wire surface loose and form ripples along the scanning direction as shown in Fig. 3a. So appropriate laser powers ranging from 5 mW to 10 mW were chosen to adjust the wire width and ensure a continuous surface.

The resistivity of the laser-created wires was measured, for which we designed two Au–Ge–Ni electrodes coated on a cover glass substrate with a slit of 100 μm by physical vapor evaporation technology as shown in Fig. 3c. Subsequently, three gold wires were patterned between the two electrodes in parallel. A series of voltages was applied to the two electrodes and the current–voltage curve of gold wires exhibits a linear dependence. The electrical resistivity was measured to be $\sim 5.5 \times 10^{-8}$ Ω m (details shown in Fig. S1†), only 2 times larger than that of bulk gold (2.4×10^{-8} Ω m). It has been stable for two months since it was created, different from the resistivity of silver microwires which changed after one day (Fig. S2†).

Laser can not only pattern gold nanodots on a glass surface, but also on polymer film. In order to verify the technical feasibility of interconnecting nanospecies located randomly on a surface with the metal wires, we designed a simple bottom gate multiwall carbon nanotube field effect transistor (MWCNT-FET). Different from the general method of introduction of nanotubes on a prepared electrode pair, a process difficult to control, here we chose to start with nanotubes in the proper position and then induced the leads by the laser deposition of Au nanodots to construct the FET. The bottom-gate device structure diagram is shown in Fig. 4a. A film of 200 nm thick SU-8 polymer was used as insulation layer, the gold electrodes were 100 nm thick and an ITO film with 80 nm thickness was applied as bottom gate. The laser patterned gold leads show good compatibility with the single CNT on the polymer substrate. The SEM of gold leads connecting a 19 μm long MWCNT on a SU-8 polymer is shown in Fig. 4c and the CNT between the 1.5 μm wide gold leads is also distinguished through element distribution mapping SEM (Fig. 4d) and energy dispersive X-ray mapping spectrum (Fig. 4e). Fig. 4b shows a set of typical current *versus* source drain voltage (I_{DS}–V_{DS}) curves obtained from an individual MWCNT-FET at different gate voltages (V_G) in air. With increasing the value of V_G, the source–drain current was increased at the source–drain bias of −10 V. The result indicates that this device showed n-type characteristics in air.

Conclusion

In conclusion, we firstly developed a method of patterning gold micronanostructures using nanodots precursor instead of metal ions by tight focused femtosecond laser direct writing. The stable gold structures possess high conductivity that is comparable to the bulk material, thus making it a novel approach for interconnecting nanospecies like single MWCNTs on arbitrary substrates, especially as no electrodes could be prepared that would be compatible for connecting random MWCNTs. We think that laser patterning conductive gold micronanostructures from nanodots would be of benefit for developments of functional layered architectures of various nanomaterials[17] and would form another construction strategy of thin-film-based nanoarchitectures.[18]

Acknowledgements

The authors gratefully acknowledge the financial support from the National Science Foundation of China (Grant no. 90923037, 61008014 and 6078048). The work was also supported by 2010 PhD interdisciplinary project no. 450091102507, Jilin University.

Published on 28 August 2012 on http://pubs.rsc.org | doi:10.1039/C2NR31614E
Downloaded by Jilin University on 31 October 2012

View Online

Notes and references

1 B. M. Ross, L. Y. Wu and L. P. Lee, *Nano Lett.*, 2011, **11**, 2590.
2 Y. Choi, Y. Park, T. Kang and L. P. Lee, *Nat. Nanotechnol.*, 2009, **4**, 742.
3 (*a*) Z. Zhu, H. Meng, W. Liu, X. Liu, J. Gong, X. Qiu, L. Jiang, D. Wang and Z. Tang, *Angew. Chem.*, 2011, **123**, 1631; (*b*) R. Zhang, B.-B. Xu, X.-Q. Liu, Y.-L. Zhang, Y. Xu, Q.-D. Chen and H.-B. Sun, *Chem. Commun.*, 2012, **48**, 5913; (*c*) B.-B. Xu, Z.-C. Ma, H. Wang, X.-Q. Liu, Y.-L. Zhang, X.-L. Zhang, R. Zhang, H.-B. Jiang and H.-B. Sun, *Electrophoresis*, 2011, **32**, 3378.
4 K. K. R. Datta, B. V. S. Reddy, K. Ariga and A. Vinu, *Angew. Chem.*, 2010, **122**, 6097.
5 D. Liu, Z. Wang and X. Jiang, *Nanoscale*, 2011, **3**, 1421.
6 K. Ariga, X. Hu, S. Mandal and J. P. Hill, *Nanoscale*, 2010, **2**, 198.
7 J. Kim, J. You, B. Kim, T. Park and E. Kim, *Adv. Mater.*, 2011, **23**, 4168.
8 (*a*) S. Kawata, H.-B. Sun, T. Tanaka and K. Takada, *Nature*, 2001, **412**, 697; (*b*) K. Ueno, S. Juodkazis, T. Shibuya, Y. Yokota, V. Mizeikis, K. Sasaki and H. Misawa, *J. Am. Chem. Soc.*, 2008, **130**, 6928; (*c*) J. Wang, H. Xia, B.-B. Xu, L.-G. Niu, D. Wu, Q.-D. Chen and H.-B. Sun, *Opt. Lett.*, 2009, **34**, 581; (*d*) Y.-Y. Cao, N. Takeyasu, T. Tanaka, X.-M. Duan and S. Kawata, *Small*, 2009, **5**, 1144; (*e*) T. Tanaka, A. Ishikawa and S. Kawata, *Appl. Phys. Lett.*, 2006, **88**, 081107.
9 (*a*) A. Ishikawa, T. Tanaka and S. Kawata, *Appl. Phys. Lett.*, 2006, **89**, 113102; (*b*) B.-B. Xu, Z.-C. Ma, L. Wang, R. Zhang, L.-G. Niu, Z. Yang, Y.-L. Zhang, W.-H. Zheng, B. Zhao, Y. Xu, Q.-D. Chen, H. Xia and H.-B. Sun, *Lab Chip*, 2011, **11**, 3347; (*c*) L.-L. Qu, D.-W. Li, J.-Q. Xue, W.-L. Zhai, J. S. Fossey and Y.-T. Long, *Lab Chip*, 2012, **12**, 876; (*d*) B.-B. Xu, H. Xia, L.-G. Niu, Y.-L. Zhang, K. Sun, Q.-D. Chen, Y. Xu, Z.-Q. Lv, Z.-H. Li, H. Misawa and H.-B. Sun, *Small*, 2010, **6**, 1762.
10 L. Vurth, P. Baldeck, O. Stephan and G. Vitrant, *Appl. Phys. Lett.*, 2008, **92**, 171103.
11 X. Zhang, B. Sun, R. H. Friend, H. Guo, D. Nau and H. Giessen, *Nano Lett.*, 2006, **6**, 651.
12 Y. Zhao, Z. Wang, W. Zhang and X. Jiang, *Nanoscale*, 2010, **2**, 2114.
13 Y.-L. Sun, W.-F. Dong, R.-Z. Yang, X. Meng, L. Zhang, Q.-D. Chen and H.-B. Sun, *Angew. Chem., Int. Ed.*, 2012, **51**, 1558.
14 M. Miyazaki and Y. Hayasaki, *Opt. Lett.*, 2009, **34**, 821.
15 (*a*) K. Svoboda and S. M. Block, *Opt. Lett.*, 1994, **19**, 930; (*b*) F. Hajizadeh and S. N. S. Reihani, *Opt. Express*, 2010, **18**, 551.
16 A. S. Urban, A. A. Lutich, F. D. Stefani and J. Feldmann, *Nano Lett.*, 2010, **10**, 4794.
17 K. Ariga, Q. Ji, J. P. Hill, Y. Bando and M. Aono, *NPG Asia Mater.*, 2012, **4**, e17.
18 K. Sakakibara, J. P. Hill and K. Ariga, *Small*, 2011, **7**, 1288.

Published on 28 August 2012 on http://pubs.rsc.org | doi:10.1039/C2NR31614E
Downloaded by Jilin University on 31 October 2012

This journal is © The Royal Society of Chemistry 2012